Biodegradable star-shaped poly(lactic acid): Synthesis, characterization and its reaction kinetics

Jing He[a], Tao Yu[a,b*], Weidong Yang[a], Yan Li[a]
a. School of Aerospace Engineering and Applied Mechanics, Tongji University, 1239 Siping Road, Shanghai, 200092, P. R. China
b. Shanghai Key Laboratory for Planetary Mapping and Remote Sensing for Deep Space Exploration, Tongji University, 1239 Siping Road, Shanghai, 200092, P. R. China

Abstract

Biodegradable four-arm star-shaped poly(lactic acid) (4sPLA) was synthesized from $_{L}$-Lactic acid ($_{L}$-LA) and pentaerythritol (PENTA), and the polymerization kinetics was studied. The effects of reaction time, reaction temperature and molar ratio on the polymerization of 4sPLA were discussed. The molecular structure of 4sPLA was characterized by Fourier transform infrared spectroscopy (FTIR) and ^{1}H nuclear magnetic resonance spectra (^{1}H-NMR). The results showed that the optimum reaction conditions were as follows: the molar ratio of $_{L}$-LA to PENTA was 12:1, and the polymerization reaction occurred at 160 ℃ for 5 h. Gel permeation chromatography (GPC) method was used to determine the polymerization kinetics of 4sPLA consistent with the first-order reaction kinetics.

Keywords

star-shaped poly(lactic acid); biodegradable; polymerization kinetics; optimum reaction conditions

* Corresponding author at: School of Aerospace Engineering and Applied Mechanics, Tongji University, No.1239 Siping Road, Shanghai 200092, PR China. Tel.:+86 21 65980239; Fax: +86 21 65983950. E-mail address: yutao@tongji.edu.cn (T. Yu)

Introduction

Due to the environmental issues and biomedical applications, biodegradable and biocompatible polymers have attracted the attention of many researchers. Poly(lactic acid) (PLA) as a non-petroleum biodegradable polymer is mainly obtained from renewable crops [1, 2]，which can be completely degraded into carbon dioxide and water in nature conditions [3-5]. It is widely used in biomedical, agricultural, food and other fields because of the advantages of biocompatibility and good mechanical properties [6-9]. In recent years, a variety of branched fractal structures, such as grafting, star and cross-linking, have been proposed to further improve the performance of PLA [10-14]. Moreover, more researchers are interested in studying on the synthesis, properties and applications of star-shaped PLA with unique spatial structure [15].

Star-shaped PLA has the properties of lower viscosity, controllable degradation period and better melt fluidity which can be applied in biocomposites, biomedical, drug delivery and smart packaging areas [16-18]. Star-shaped PLA is formed by the polymerization of multifunctional core molecule and PLA chain[13]. The "core first" method is usually utilized to synthesize star-shaped PLA [19]. Current researches are mainly about small molecular polyhydroxyl alcohols, metal-organic compounds and other different types of "core" to synthesis of star-shaped PLA. Yuan et al. [20] used 4-dimethylaminopyridine as catalyst to catalyze ring-opening polymerization of $_{L}$-lactide with pentaerythritol (PENTA) or dipentaerythritol (DPE) to obtain four-arm star-shaped poly(lactic acid) (4sPLA) or six-arm star poly(lactic acid) (6sPLA).

Jessica et al. [21] prepared the iron tris(dibenzoylmethane) (dbm)-centered PLA stars ($Fe(dbmPLA)_3$) by ring-opening polymerization of $_L$-lactide with $Fe(dbmOH)_3$ as initiator. Tsuji et al. [22] synthesized three-arm star-shaped PLA with glycerol as "core" and $_L$-lactide as raw material.

The reaction rate of the synthesis of polymers is very important since it will influence the final industrial production efficiency [23, 24]. Therefore, it is necessary to study the polymerization reaction kinetics of star-shaped PLA to improve the reaction efficiency and optimize the synthesis process. Recently, different methods were used to analyze the reaction kinetics of linear PLA and star-shaped PLA. Dimas A. et al. [25] used ^{1}H nuclear magnetic resonance spectra (^{1}H-NMR) method to monitor the end-group concentration at different reaction periods, and the results showed that the polymerization reaction of $_L$-LA monomer was first-order. Scott J et al. [26] found the reaction kinetics of PENTA and $_L$-LA in the polymerization process was consistent with the first-order reaction kinetics by mid-infrared attenuated total reflectance-Fourier transform infrared (ATR-FTIR) spectroscopy. Karina A. et al. [27] studied the polymerization kinetics of 4sPLA and established the first-order reaction kinetics model by using *in-situ* FT-Raman spectroscopy.

However, most studies on the reaction kinetics of star-shaped PLA are focused on high molecular weight star-shaped PLA, but there are few studies on the reaction kinetics of low molecular weight star-shaped PLA. Compared with high molecular weight star-shaped PLA, low molecular weight star-shaped PLA has a lower resin viscosity and can improve the processability of the resin. With the

end-functionalization of PLA chain, low molecular weight star-shaped PLA can obtain cross-linkable products, which can be used as a resin matrix and natural fiber to prepare low-cost, environmental biocomposites [28-30]. To study the reaction kinetics of the synthesis process of star-shaped PLA will improve the reaction efficiency, which can reduce energy consumption and cost during the process of production. Moreover, it will be helpful for accelerating the industrialization development of low molecular weight PLA and its cross-linkable products, and expanding the range of applications in the field of biomedical and biocomposites.

The purpose of this study is to investigate the reaction kinetics of low molecular weight 4sPLA resin and provide a theoretical basis for the control of reaction process to simplify the process and reduce the production cost. In this paper, we explored the optimum reaction conditions of low molecular weight 4sPLA resin by studying the effects of reaction time, reaction temperature and molar ratio on the polymerization reaction. The molecular structure of low molecular weight 4sPLA was determined by Fourier transform infrared (FTIR) and ^{1}H-NMR. Gel permeation chromatography (GPC) method which could measure molecular weight directly was utilized to evaluate the reaction kinetics model and E_a of 4sPLA.

Experiment

Materials

L-LA (85%) and stannous octoate as catalyst were purchased from Sinopharm Chemical Reagent Co., Ltd., China. PENTA was used as the initiator and dried at 50 ℃ for 12 h before use, which was obtained from Aladdin Reagent Co., Ltd., China.

Synthesis of 4sPLA

The synthetic route is shown in Fig. 1. $_{L}$-LA was dehydrated to obtain $_{L}$-lactide at 90 ℃ for 2 h by circulating water vacuum pump. Then, the 4sPLA with branched chain length of 2 was synthesized with 12:1 molar ratio of $_{L}$-lactide to PENTA. The stannous octoate was used as catalyst (0.1 wt %) at 160 ℃ for 5 h under a nitrogen atmosphere.

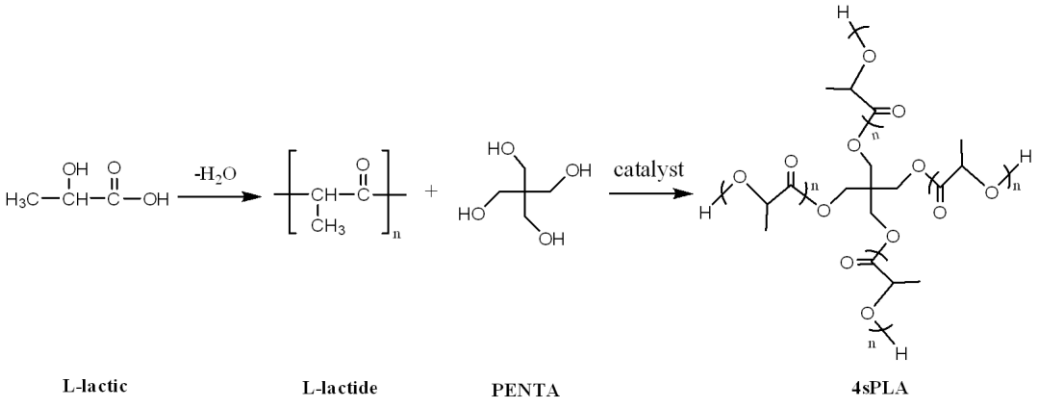

Fig. 1 The synthetic route of 4sPLA

Characterization

^{1}H-NMR spectra was recorded with a Bruker DMX-500 NMR spectrometer in deuterium dimethyl sulfoxide (DMSO) solvent and tetramethylsilane (TMS) as the internal standard at room temperature. FTIR spectra was measured with a Nicolet 6700 FTIR spectrometer at room temperature. The sample/KBR with a mass ratio of 1:100~1:200 was evenly mixed and pressed into sheets. The scanning range was from 4000 to 400 cm^{-1} with a resolution of 4 cm^{-1}.

GPC analysis was performed on an Agilent 1260 Infinity to record the average molecular weight and molecular weight distribution. Polymer samples were dissolved in mobile phase tetrahydrofuran (THF) at a flow rate of 0.7 $mL \cdot min^{-1}$.

The temperature of the inner column was always maintained at 35 ℃ with polystyrene (PS) as a standard sample. The molecular weight of the samples was measured by GPC method and the samples were obtained at different reaction times of 0.5, 1, 2, 3, 4 and 5 h.

Results and Discussion

^{1}H-NMR analysis

^{1}H-NMR spectra of 4sPLA is shown in Fig. 2. The multiple peaks at 1.50 ~ 1.58 ppm (a) and 5.10 ~ 5.15 ppm (b) were assigned to branched chain methyl protons and methane protons respectively. The ratio of peak area of peak (a) to peak (b) was 3:1. The peak at 3.30 ~ 3.35 ppm (d) corresponded to the terminal O-H groups in 4sPLA arms. Compared to the characteristic peaks of linear PLA, the specific peak of methylene protons which assigned to terminal O-H group in the initiator PENTA linked to PLA chain was at 4.20 ~ 4.33 ppm (c), and the ratio of peak area of peak (b) to peak (c) was close to 1:2. All the above characteristic peaks could be ascribed to the molecular structure of the target product, which indicated that the product 4sPLA was successfully synthesized.

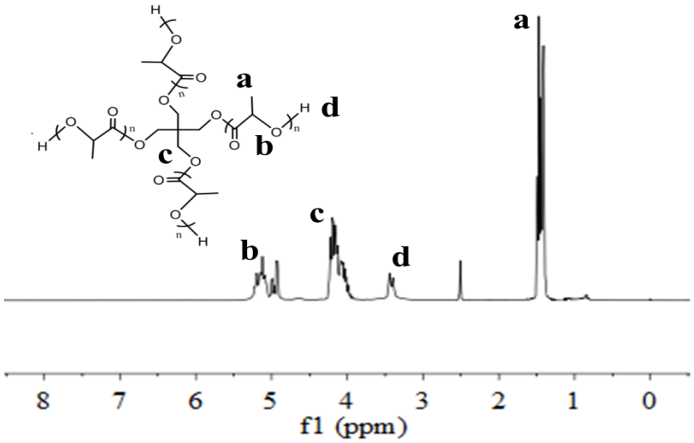

Fig. 2 The ^{1}H-NMR spectra of 4sPLA

FTIR analysis

The chemical structures of linear PLA and 4sPLA were determined by FTIR spectra (as shown in Fig. 3). The band at 3558 cm^{-1} was attributed to the characteristic peak of terminal oxhydryl (O-H) group. The bands at 2992 cm^{-1}, 1944 cm^{-1}, 2937 cm^{-1} represented the methyl group ($-CH_3$), carbonyl group (C=O) and methine group (-CH), respectively. After the reaction with the initiator PENTA, the stretching vibration peak appeared at 980 cm^{-1} corresponded to C-O-C which represent the initiator terminus connected to the linear PLA carbonyl group. Another new band could be observed at 2875 cm^{-1} (stretching, $-CH_2$). Combined with the analysis of ^{1}H-NMR spectra, FTIR further confirmed the successful functionalization of the product 4sPLA.

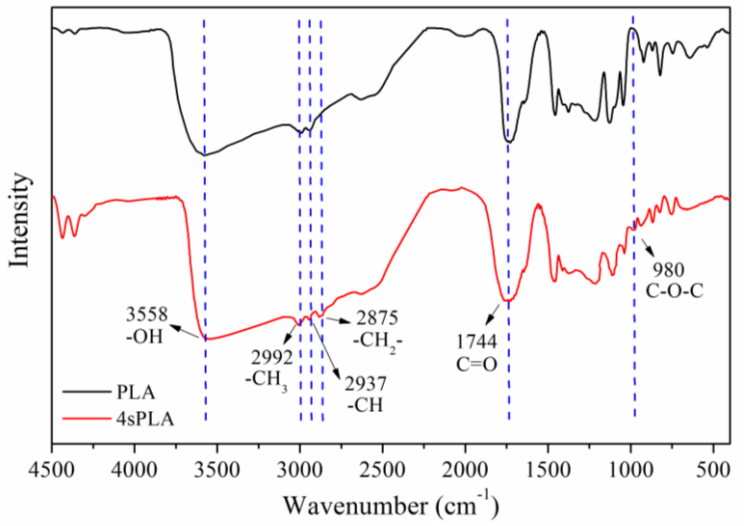

Fig. 3 The FTIR spectra of 4sPLA

Effect of reaction conditions on polymerization reaction

The synthesis of polymers involves some reaction conditions (reaction time, reaction temperature, and the molar ratio of raw materials, etc.). Once a certain reaction condition is changed, the properties of the product will be affected. For the

polymerization reaction of star-shaped PLA, these reaction conditions can seriously affect the reaction activity of the reactants, the reaction rate, the degree of reaction and the molecular weight [31]. In order to obtain the optimal synthesis process of the target product, the reaction conditions needed to be designed and screened. In this study, the single-factor control variable method was utilized to investigate the optimal reaction conditions of star-shaped PLA.

In Fig. 4, when the reaction time exceeded 5 h, the number average molecular weight (M_n) increased, but the decrease of $_L$-lactide concentration led to a decrease of the reaction rate with the reaction time longer. At the same time, with the increase of reaction time, the viscosity of the reaction system increased, which resulted in by-products such as water difficult to be expelled and molecular weight distribution (PDI) wider [32, 33]. In addition, as the reaction time increased, for the target product, the molecular weight was much higher than the theoretical molecular weight, which meant that PLA chains had reacted with more small molecules and would increase the steric hindrance of molecular microstructure resulting in hinder the further end-functionalization reaction of the target product [13]. Based on the analysis, 5 h selected as the reaction time was more appropriate.

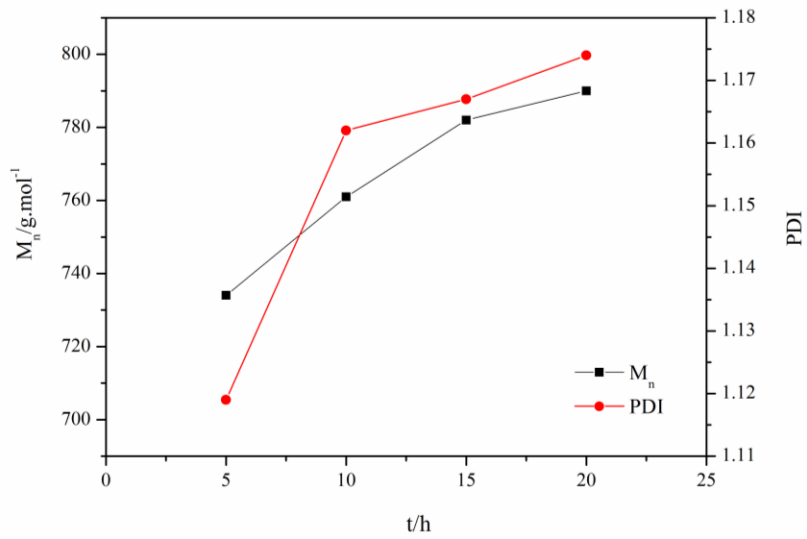

Fig. 4 Effect of reaction time on M_n and PDI

As shown in Fig. 5, the molecular weight of 4sPLA was greatly affected by temperature. When the reaction temperature was lower than 160 ℃, the molecular chain moved slowly at the low temperature, which caused the insufficient reaction and low molecular weight. With the reaction temperature over 160 ℃, the molecular chain movement accelerated and the molecular weight increased obviously. However, the color of 4sPLA resin darkened which was a result of generated side reactions such as hydrolysis, thermal degradation and carbonization in the reaction process under high temperature conditions [34]. It was suggested that 160 ℃ could be chosen as the reaction temperature.

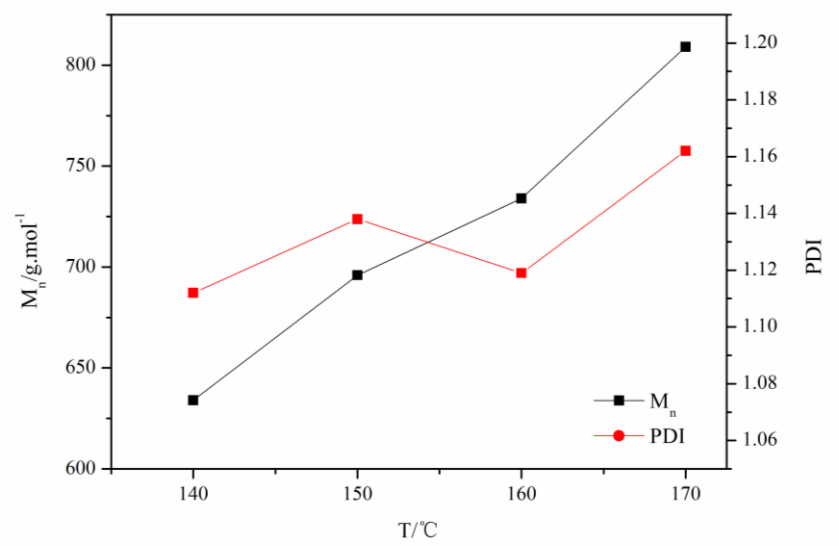

Fig. 5 Effect of reaction temperature on M_n and PDI

Fig. 6 showed the effects of molar ratio on polymerization reaction. The molecular weight increased with the increase of the molar ratio of $_L$-LA to PENTA. It could be analyzed that the increased molar ratio of $_L$-LA to PENTA led to the number of $_L$-LA monomers corresponding to the reaction active site larger and the molecular weight increased [35]. When the molar ratio was up to 12:1, the molecular weight distribution was the narrowest. Compared with the molar ratio of 12:1, the molecular weight at a molar ratio of 14:1 was significantly increased. Moreover, in consideration of saving raw material costs, 4sPLA polymerized with 12:1 mole ratio of $_L$-LA to PENTA could be conducted more appropriately.

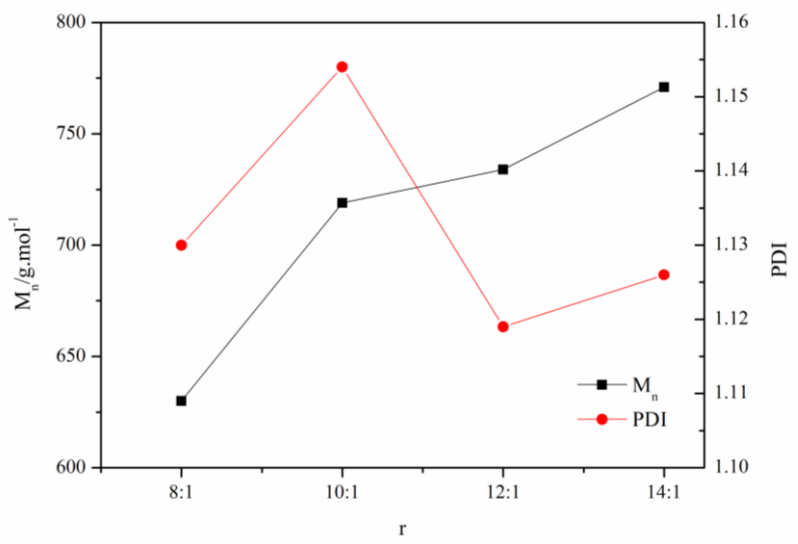

Fig. 6 Effect of molar ratio on M_n and PDI

According to the above analysis of the reaction conditions (temperature, time, and mass ratio) on the synthesis of 4sPLA, the reaction temperature has a distinct effect on the molecular weight of 4sPLA. Under the conditions that the ratio of $_L$-LA to PENTA was 12:1, the synthesis of 4sPLA took place at a temperature of 160 ℃ for 5 h, which was the optimum reaction conditions for star-shaped PLA.

Reaction kinetics analysis

In order to determine the reaction order of $_L$-LA in the process of synthesizing low molecular weight 4sPLA resin, the kinetic reaction was completed under the optimal conditions obtained by a single-factor control variable method. The polymerization reaction of 4sPLA resin can be calculated according to the kinetics equation shown in equation (1):

$$-\frac{\mathrm{d}[\mathrm{M}]}{\mathrm{d}t} = k[\mathrm{M}]^n[\mathrm{PET}]^a[\mathrm{CAT}]^b \quad (1)$$

where $[\mathrm{M}]$ is $_L$-LA monomer concentrations, $[\mathrm{PET}]$ is PENTA concentrations and $[\mathrm{CAT}]$ is catalyst concentrations; n, a and b are the reaction orders of

$[\mathrm{M}]$, $[\mathrm{PET}]$ and $[\mathrm{CAT}]$, respectively. k is the rate constant of the polymerization reaction. The volume of the reaction system can be assumed unchanged with time which is due to the polymerization reaction at a constant temperature and the assumption of no material discharge and loss in the whole reaction process. The reaction order n of L-LA can be determined by k set as $k_s = k[\mathrm{PET}]^a[\mathrm{CAT}]^b$. The kinetic equation (1) can be converted into:

$$-\frac{\mathrm{d}[\mathrm{M}]}{\mathrm{d}t} = k_s[\mathrm{M}]^n \tag{2}$$

The reaction order n can be determined according to the relationship between the reaction time and the conversion. The curve of molecular weight versus conversion under the optimal reaction conditions is shown in the Fig. 7. As can be seen from the figure, the molecular weight increased with the increase of conversion and they have a good linear relationship. The highest conversion reached 96.3%.

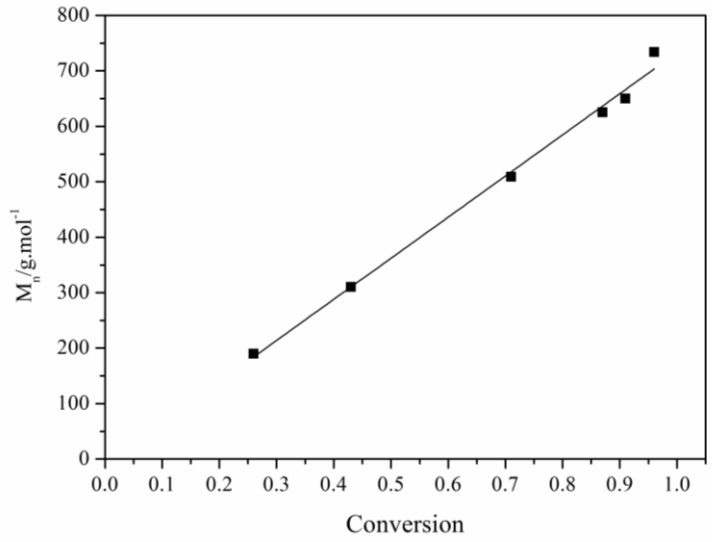

Fig. 7 The plot of conversion versus time

When $n = 1$, equation (2) can be converted to equation (3):

$$-\frac{\mathrm{d}[\mathrm{M}]}{\mathrm{d}t}=k_s[\mathrm{M}] \tag{3}$$

Equation (4) can be obtained by integrating equation (3):

$$-k_s t=\ln\frac{[\mathrm{M}]}{[\mathrm{M}]_0} \tag{4}$$

The conversion x is calculated by the molecular weight measured by GPC method. The end group concentration ($\mathrm{mol/g}$) of the reaction solution is defined in terms of mass. According to the definition of conversion, the calculation equation of x is shown as equation (5):

$$x=1-\frac{[\mathrm{M}]}{[\mathrm{M}]_0} \tag{5}$$

where $[\mathrm{M}]$ is the mass concentration of the reactants at different times, $[\mathrm{M}]_0$ is the initial mass concentration of the reactants.

Equation (5) is substituted into equation (4) to obtain equation (6):

$$k_s t=\ln\frac{1}{1-x} \tag{6}$$

Fig. 8 shows the linear fitting curve with $\ln\left(\frac{1}{1-x}\right)$ versus time (t), and the linear correlation coefficient (R^2) is 0.9931.

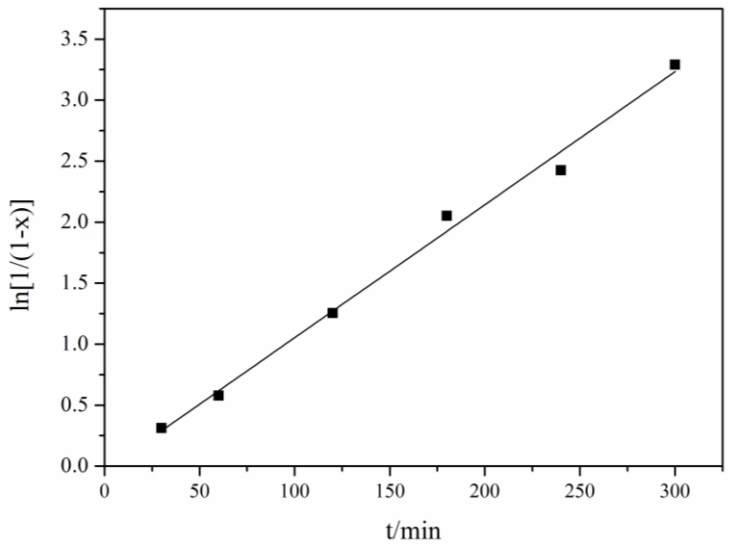

Fig. 8 The first-order fitting curve of the reaction

When $n = 2$, equation (7) can be obtained from equation (2):

$$-\frac{\mathrm{d}[\mathrm{M}]}{\mathrm{d}t} = k_s [\mathrm{M}]^2 \tag{7}$$

Integrate equation (7) to obtain equation (8):

$$k_s t = \frac{1}{[\mathrm{M}]} - \frac{1}{[\mathrm{M}]_0} \tag{8}$$

Ibid., equation (8) can be transformed into equation (9) :

$$[\mathrm{M}]_0 k_s t = \frac{1}{1-x} - 1 \tag{9}$$

R^2 (0.8262) can be obtained from the linear fitting curve with $1/(1-x)$ versus time (t) as shown in Fig. 9.

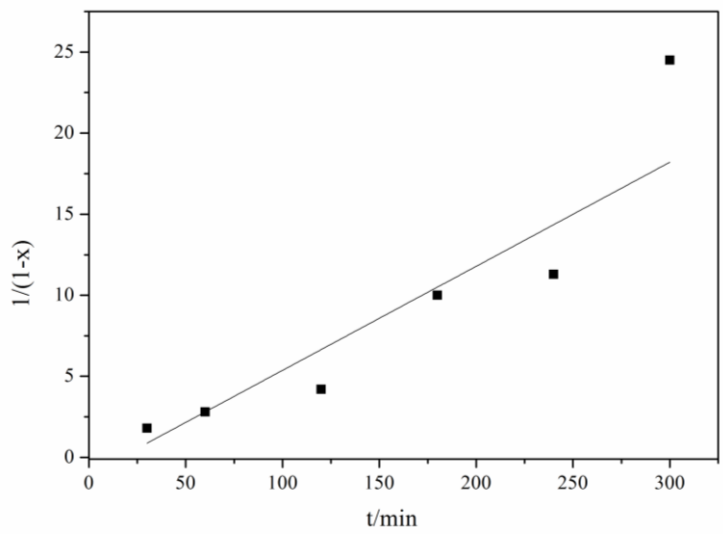

Fig. 9 The second-order fitting curve of the reaction

When $n=3$, equation (10) can be obtained from equation (2):

$$-\frac{\mathrm{d}[\mathrm{M}]}{\mathrm{d}t}=k_s[\mathrm{M}]^3 \tag{10}$$

Equation (11) can be obtained by integrating equation (10):

$$\alpha k_s t=\frac{1}{[\mathrm{M}]^2}-\frac{1}{[\mathrm{M}]_0^2} \tag{11}$$

Equation (12) is further transformed by equation (11):

$$\alpha[\mathrm{M}]_0^2 k_s t=\frac{1}{(1-x)^2}-1 \tag{12}$$

The fitting curve with $1/(1-x)^2$ versus time (t) is shown in Fig. 10. It can be seen that the fitting curve is nonlinear and the result doesn't conform to the polymerization process of the reaction.

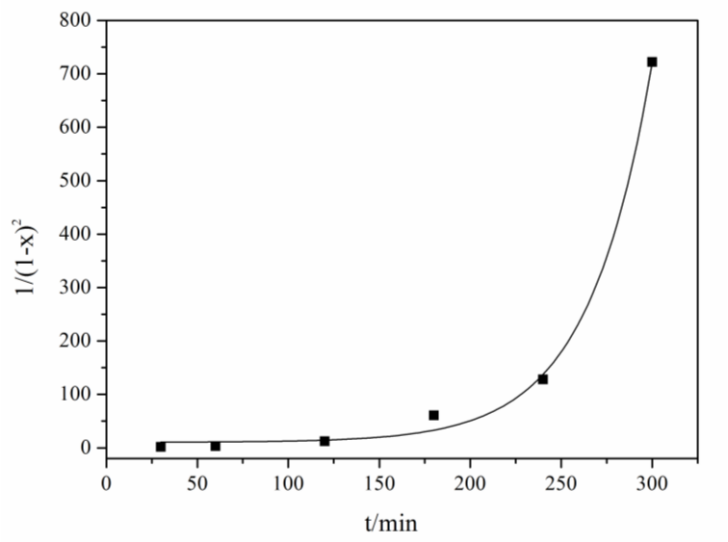

Fig. 10 The third-order fitting curve of the reaction

Based on the above results, when the reaction is modeled in first-order kinetics, the linear correlation coefficient (R^2) is close to 1, which indicates that the reaction is a first-order reaction. The order of the reaction kinetics is consistent with the first-order kinetics of the polymerization of star-shaped PLA as reported in literature [26]. According to the slope of the curve shown in Fig. 8, the reaction rate constant (k) of 4sPLA resin is 0.0109 min^{-1}.

In order to further verify the correctness of the reaction kinetics equation and reaction rate constant, k was substituted into equation (6) and the simulated value of conversion x^* was obtained by integrating equation (6). The simulated value curve is shown in Fig. 11. It can be seen that the experimental value of conversion x is in good agreement with the simulation calculation curve of the dynamics model. The correlation coefficient (R^2) is 0.9882 and the relative error between the experimental value and simulation value is less than 1 %, which proves that the first-order reaction kinetic model obtained in the study is correct.

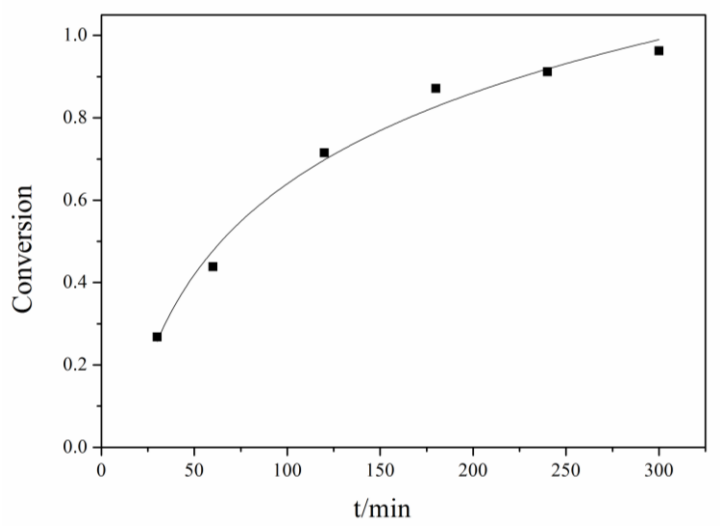

Fig. 11 The simulation verification curve of the experimental value

The reaction activation energy (E_a) reflects the effect of temperature on the reaction rate constant. E_a is calculated by Arrhenius equation (13) as follows:

$$k = A_0 \exp\left(-\frac{E_a}{RT}\right) \tag{13}$$

where E_a is activation energy; A_0 is the pre-exponential factor; R is the universal gas constant; T is the Kelvin temperature. Equation (14) can be obtained by taking the logarithm of both ends of equation (13):

$$\ln k = -\frac{E_a}{RT} + \ln A_0 \tag{14}$$

In order to determine E_a, the reaction rate constant at different temperatures (140, 150, 160, 170 ℃) should be calculated. The linear fitting curves and the calculate results were shown in Fig. 12 and Table 1, respectively. Then rate constants values were plotted in an Arrhenius diagram (as shown in Fig. 13). It can be seen from Fig. 13 that $\ln k$ and $1/T$ have a linear relationship. The linear fitting equation is $\ln k = -4336.5/T + 1.3561$, E_a obtained according to the slope is 36.1 kJ/mol. In addition, it can be found from Fig. 12 and Table 1 that for the same system, the

reaction rate constant increases with the increase of reaction temperature. It is suggested that the increase in temperature causes a decrease in the viscosity of the reaction system, an increase in activity of chain reaction and the reaction rate accelerate, leading to the increase in the reaction rate constant.

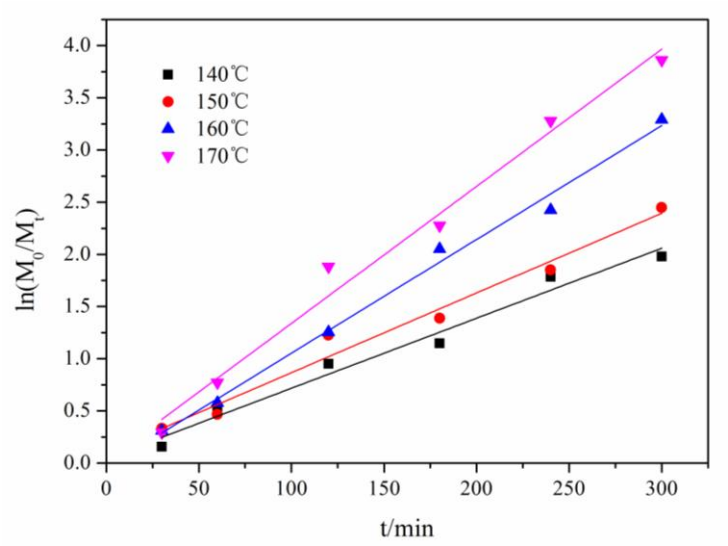

Fig. 12 The linear fitting curves at different temperatures (140, 150, 160, 170 ℃)

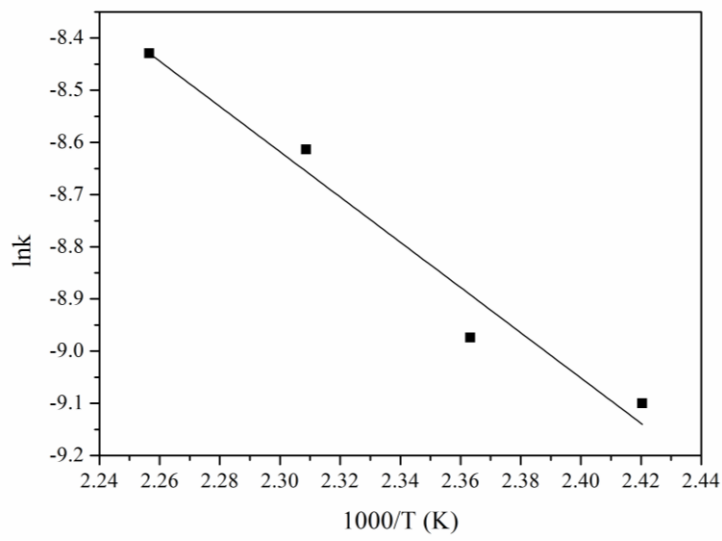

Fig. 13 The Arrhenius plot of k values at different temperatures (140, 150, 160, 170 ℃)

Temperature/℃	k / $\min^{-1}$	R^2
140	0.0067	0.9785
150	0.0076	0.9787
160	0.0109	0.9931
170	0.0131	0.9863

Table 1 The k and R^2 at different temperatures (140, 150, 160, 170 ℃)

Conclusion

Low molecular weight 4sPLA resin was successfully prepared by using stannous octoate as catalyst, PENTA as initiator and $_{\text{L}}$-LA as raw material. The effects of different reaction conditions (reaction time, reaction temperature, feed ratio) were studied by a single-factor control variable method. The optimal reaction conditions were obtained as follows: 4sPLA was polymerized with 12:1 mole ratio of $_{\text{L}}$-LA to PENTA at a temperature of 160 ℃ for 5 h. The reaction kinetics of 4sPLA and the reaction kinetics parameters at different reaction temperatures were examined by means of GPC method. The results showed that the reaction kinetics model of 4sPLA matched the first-order reaction kinetics, the reaction rate constant (k) is 0.0109 $\min^{-1}$ and the Arrhenius equation was $\ln k = -4336.5/T + 1.3561$. The reaction kinetics results have theoretical guiding significance for the exploration of the influencing factors of the reaction, the optimization of experimental conditions and the improvement of the industrial production efficiency of star-shaped PLA.

Acknowledgements

This work is supported by National Natural Science Foundation of China (No. 11872279, No. 12172258 and No. 11625210) and Natural Science Foundation of

Shanghai (No. 18ZR1440700).

References

1. Norazlina H, Kamal Y (2015) Polym Bull 72: 931-961.
2. Garlotta D (2001) J Polym Environ 9: 63-84.
3. Zaaba N F, Jaafar M (2020) Polym Eng Sci 60: 2061-2075.
4. Braun B, Dorgan J R, Knauss D M (2006) J Polym Environ 14: 49-58.
5. Abu Ghalia M, Dahman Y (2018) J Polym Environ 26: 1903-1919.
6. Liao Q H, Peng X F, Fang H, Turng L S, Huang A, Chang C C (2020) J Polym Environ 28: 295-303.
7. Jiang N, Yu T, Li Y, Pirzada T J, Marrow T J (2019) Compos Sci Technol 173: 15-23.
8. Burgos N, Tolaguera D, Fiori S, Jimenez A (2014) J Polym Environ 22: 227-235.
9. Zheng L, Geng Z X, Zhen W J (2019) J Polym Res 26: 78.
10. Chen P, Yu K S, Wang Y Q, Wang W B, Zhou H F, Li H Q, Mi J G, Wang X D (2018) J Polym Environ 26: 3718-3730.
11. Shin B Y, Han D H, Narayan R (2010) J Polym Environ 18: 558-566.
12. Michalski A, Brzezinski M, Lapienis G, Biela T (2019) Prog Polym Sci 89: 159-212.
13. Jahandideh A, Muthukumarappan K (2017) Eur Polym J 87: 360-379.
14. Hachana N, Wongwanchai T, Chaochanchaikul K, Harnnarongchai W (2017) J Polym Environ 25: 323-333.
15. Yan X Q, Li J B, Ren T B (2018) E-Polymers 18: 559-568.
16. Jing Z X, Shi X T, Zhang G C (2016) Polym Composite 37: 2744-2755.
17. Lee S H, Kim S H, Han Y K, Kim Y H (2001) J Polym Sci Pol Chem 39: 973-985.
18. Esmaeili N, Jahandideh A, Muthukumarappan K, Akesson D, Skrifvars M (2017) J Appl Polym Sci 134: 45341.
19. Cameron D J A, Shaver M P (2011) Chem Soc Rev 40: 1761-1776.
20. Yuan M W, He Z G, Li H L, Jiang L, Yuan M L (2014) Polym Bull 71: 1331-1347.
21. Gorczynski J L, Chen J B, Fraser C L (2005) J Am Chem Soc 127: 14956-14957.
22. Tsuji H, Miyase T, Tezuka Y, Saha S K (2005) Biomacromolecules 6: 244-254.
23. Costa L I, Tancini F, Hofmann S, Codari F, Trommsdorff U (2016) Macromol Symp 360: 40-48.
24. Chu S L, Li X, Robertson A W, Sun Z Y (2021) Acta Phys-Chim Sin 37: 2009023.
25. Medina D A, Contreras J M, Lopez-Carrasquero F J, Cardozo E J, Contreras R R (2018) Polym Bull 75: 1253-1263.
26. Moravek S J, Messman J M, Storey R F (2009) J Polym Sci Pol Chem 47: 797-803.
27. George K A, Schue F, Chirila T V, Wentrup-Byrne E (2009) J Polym Sci Pol Chem 47: 4736-4748.
28. Akesson D, Skrifvars M, Seppala J, Turunen M, Martinelli A, Matic A (2010) J Appl Polym Sci 115: 480-486.
29. Jahandideh A, Muthukumarappan K (2016) Eur Polym J 83: 344-358.
30. Bakare F O, Ramamoorthy S K, Akesson D, Skrifvars M (2016) Compos Part a-Appl S 83: 176-184.
31. Zhao Y L, Qing C, Jing J, Shuai X T, Bei J Z, Chen C F, Fu X (2002) Polymer 43: 5819-5825.

32. Ehsani M, Khodabakhshi K, Asgari M (2014) E-Polymers 14: 353-361.
33. Eldessouki M, Buschle-Diller G, Gowayed Y (2016) Des Monomers Polym 19: 180-192.
34. Kundys A, Plichta A, Florjanczyk Z, Zychewicz A, Lisowska P, Parzuchowski P, Wawrzynska E (2016) Polymer International 65: 927-937.
35. Nagahama K, Ohya Y, Ouchi T (2006) Polym J 38: 852-860.